

Estimating surface water and vadose water resources for an ungauged inland catchment in Vietnam

Liem Duy Nguyen, Phuong Dong Nguyen Dang and Loi Kim Nguyen

ABSTRACT

This study aimed to assess water resources for the La Vi catchment, an ungauged inland basin in Vietnam. An Internet of Things-based automatic meteorological station has been installed in the catchment to record hourly weather data from 2016. By comparing water level observations with limited discharge measurements, discharges from November 2015 to February 2018 were calculated at Tan Hoa bridge using the slope-area method. The Soil and Water Assessment Tool was calibrated and validated for the wet season of 2015 and 2017, respectively, using the previously calculated water discharges. Statistical measures including Nash–Sutcliffe index, percent bias, and coefficient of determination indicated the satisfactory performance of the model in simulating water discharge on daily time steps during both periods. The results of the water resources assessment in the catchment showed that the annual average of blue water flow, green water flow, and green water storage reached 1,596.50, 371.13, and 15.36 mm, respectively. The blue water flow reached a higher value in the center of the catchment. Meanwhile, the high-value areas of green water flow and green water storage were in the western upstream and the riverside downstream. These findings could provide a valuable scientific foundation for sustainable watershed management.

Key words | blue water, green water, Internet of Things, slope-area method, Soil and Water Assessment Tool, ungauged basin

Liem Duy Nguyen

Faculty of Environment and Natural Resources,
Nong Lam University,
Ho Chi Minh City 71308,
Vietnam

Phuong Dong Nguyen Dang

Loi Kim Nguyen (corresponding author)
Research Center for Climate Change,
Nong Lam University,
Ho Chi Minh City 71308,
Vietnam
E-mail: ngkloi@hcmuaf.edu.vn

HIGHLIGHTS

- The availability and continuity of weather data in the La Vi ungauged basin have been improved by applying IoT technology.
- A systematic approach was implemented through SWAT to separately analyze the two components of water resources as blue water and green water in terms of space and time.
- Estimated discharges showed streamflow regime characteristics due to seasonal precipitation variation and weir operation.

NOTATION

Variables	Description		
95PPU	95% prediction uncertainty	ADCP	acoustic doppler current profiler
A	cross-sectional area of the flow perpendicular to the flow direction (m^2)	AGRC	perennial plants
		AGRR	other annual plants
		Arduino Uno	an open-source microcontroller board
		BARR	bare land
		CN2.mgt	SCS runoff curve number for moisture condition I
		D	water depth (m)
		DEM	digital elevation model

This is an Open Access article distributed under the terms of the Creative Commons Attribution Licence (CC BY 4.0), which permits copying, adaptation and redistribution, provided the original work is properly cited (<http://creativecommons.org/licenses/by/4.0/>).

doi: 10.2166/wcc.2021.543

DHT11	a basic, ultra low-cost digital temperature and humidity sensor	Ubidots	an IoT platform empowering innovators and industries to prototype and scale IoT projects to production
E_a	evapotranspiration on day i (mm)	URBN	built-up land
ESCO.hru	soil evaporation compensation factor	USDA	United States Department of Agriculture
FRSE	evergreen forest	WATR	water body
GW_REVAP.gw	groundwater 'revap' coefficient	w_{seep}	water entering the vadose zone from the soil profile on day i (mm)
GWQMN.gw	threshold depth of water in the shallow aquifer required for return flow to occur (mm)	Z	trend statistic in the Mann–Kendall test
H	water level (m)	β	slope estimates in the Mann–Kendall test
HRU	hydrological response unit		
HRU_SLP.hru	average slope steepness		
IoT	Internet of Things		
MODFLOW	a finite-difference groundwater flow modeling program		
n	Manning's roughness ($s/m^{1/3}$)		
NodeMCU	a low-cost open-source IoT platform		
NSI	Nash–Sutcliffe index		
OV_N.hru	Manning's ' n ' value for overland flow		
P	wetted perimeter of cross-sectional flow area (m)		
PBIAS	Percent BIAS		
p -value	the significance of sensitivity		
Q	discharge (m^3/s)		
Q_{gw}	groundwater runoff on day i (mm)		
Q_{surf}	surface runoff on day i (mm)		
r	the existing parameter value is multiplied by $(1 + \text{a given value})$		
R	hydraulic radius (m)		
R^2	coefficient of determination		
R_{day}	precipitation on day i (mm)		
REVAPMN.gw	threshold depth of water in the shallow aquifer for 'revap' to occur (mm)		
RICE	paddy rice		
S	bottom slope of channel, m/m (dimensionless)		
SLSUBBSN.hru	average slope length		
SOL_AWC(..).sol	available water capacity of the soil layer		
SWAT	Soil and Water Assessment Tool		
SW_o	the initial soil water content on day i (mm)		
SW_t	the final soil water content (mm)		
t	time (days)		
t-stat	a measure of sensitivity		

INTRODUCTION

River discharge, the volume of water passes through a river cross section per unit of time, is a spatiotemporal output of the regional hydrologic cycle. Because river flow is generally concentrated in channels, discharge can be measured with more accuracy and precision than precipitation, evapotranspiration, or any other component of the hydrologic cycle (Dingman & Bjerklie 2005). For these reasons, measurements of river discharge not only provide direct information about climate, water resource availability, and flood hazards but also make invaluable data for validating the hydrologic models that are the useful means of forecasting the impacts of land use and climate change on water resources.

Methods of measuring streamflow generally fall into four categories (Gordon et al. 2004): (1) volumetric measurement, (2) velocity-area methods involving some measure of average stream velocity and cross-sectional area, (3) dilution gauging methods using a salt or dye, and (4) stream gauging methods where water level measurements are made at natural sites or artificial control sections such as weirs, and a stage-discharge relationship is established. The selection of a good measurement site requires careful planning and evaluation. Unfortunately, in most catchments around the world, runoff is not measured directly. In these cases, streamflow can be estimated indirectly from channel characteristics. The uncertainty of Manning's roughness is the major source of error in estimating indirectly discharge in natural channels. In addition, sand-bed streams pose difficulties because flow resistance is affected by

flow-dependent bed configuration (Sefick *et al.* 2015). To overcome the above difficulties in estimating Manning's roughness, researchers have used different approaches such as optimal control theories (Ding *et al.* 2004), nonlinear optimization model (Askar & Al-Jumaily 2008), and multi-objective genetic algorithm (Reshma *et al.* 2014), combining optimization algorithm of simulated annealing with gradually varied flow equations (Heydari *et al.* 2018).

So far, there are many hydrological models developed to improve the accuracy of runoff prediction on ungauged basins. One approach to applying hydrological models in these basins is to develop a model that uses physical-based inputs varying in space and time along with comprehensiveness in the model's interrelationships and ability to predict ungauged basins reasonably well (Srinivasan *et al.* 2010). The Soil and Water Assessment Tool (SWAT) model, a free-of-charge hydrologic model, was originally developed for large-scale ungauged basins, aimed to simulate and predict the impact of land use, land management practices, and climate change on the quality and quantity of surface and groundwater in watersheds. The model has achieved international acceptance as a powerful interdisciplinary watershed-modeling tool that was tested for streamflow (Begou 2016; Ang & Oeurng 2018; Guiamel & Lee 2020; Oo *et al.* 2020), water balance (Mishra *et al.* 2017; Rafiei Emam *et al.* 2017; Sisay *et al.* 2017) in many areas around the world, especially agricultural basins.

Traditional weather monitoring systems often utilize analog weather stations that contain instruments such as anemometer, wind vane, thermometer, hygrometer, and rain gauge to measure weather changes. Most of these devices are then physically recorded and stored in a database. This information is later sent to news reporting stations and radio stations where the weather report is produced. Limitations of the above-mentioned technique are: they are bulky and inconvenient due to consisting of numerous parts that require constant maintenance, manually monitored and changed frequently; high power consumption if instruments are sited far from main power supply; manual data transfer from loggers to a computer; large occupied area; high cost of installation and maintenance; and information transmission delay to end-users (Rahut *et al.* 2018). Recently, developments in the Internet of Things (IoT) have contributed to significantly improving meteorological observation systems on

compactness, accuracy, cost-effective, and response time. IoT devices can be used to measure weather parameters anywhere and upload real-time observations to cloud storage where they can then be analyzed (Nwe & Htun 2018).

Vietnam has a dense river system consisting of about 3,450 rivers and streams with lengths of at least 10 km each. Large river basins often consist of many heterogeneous sub-basins that are hydraulically connected. Due to the sparse hydrological monitoring network with 354 existing stations (Vietnamese Government 2016) and data sharing barriers, predictions in ungauged basins have been a major challenge in managing water resources in these basins. Recent studies on this topic were conducted at Can Le catchment in Sai Gon basin (Quan 2006), upstream catchments in Huong basin (Rafiei Emam *et al.* 2017), and Ho Ho reservoir catchment in Ngan Sau basin (Kha *et al.* 2018).

In this study, we present an interdisciplinary approach that could be used to estimate water resources of the La Vi catchment, an ungauged catchment on the South Central Coast of Vietnam. First, the IoT-based weather station was established to record real-time changes in weather on the catchment. Second, continuous discharges were calculated from water level observations by the slope-area method. Finally, blue water and green water were individually quantified through a well-validated SWAT model. Compared with previous studies, the innovation of our study is to focus on improving the availability and reliability of hydro-meteorological data sources before they are included in a hydrological model to simulate physical processes. Similar studies mainly used secondary data on weather and streamflow at meteorological and hydrological stations, so data reliability could not be controlled. Meanwhile, this study installed a meteorological monitoring station and estimated streamflow directly from water level and river morphology; therefore, data reliability was assessed in detail.

METHODS

Study area

The La Vi catchment, a tributary of the Kone river basin, is located in the South Central Coast of Vietnam with an approximately 10,369 ha area and 16.5 km length as

shown in Figure 1. The catchment flows through two districts, including Phu Cat and Tay Son of Binh Dinh province. The river system originates from three main directions: North–South (Cat Trinh commune, Phu Cat district), Northwest–Southeast (Cat Hiep commune, Binh Thuan district), and South–North (Cat Tan commune, Phu Cat district) to the confluence in Ngo May town. Then, they flow in the Northwest–Southeast direction to drain into Dai An river before flowing into Thi Nai estuary.

The La Vi catchment is located on the eastern slopes of the Annamite Range with the generally inclined direction of Northwest–Southeast. Based on the terrain classification of Van Zuidam (1986), the catchment consists of flat, undulating, and hilly terrain. The elevation ranges from 7 to 362 m, with an average slope of 1.89° .

Climate in the La Vi catchment is typified by the humid tropical monsoon with an average temperature of 27°C and an average humidity of 78%. There are two distinct seasons in the year, including the dry season from January to August

and the wet season from September to December. The amount of rainfall is about 2,000 mm/year, with nearly 73% of this falling in the wet season. The two prevailing winds are the Northeast monsoon and the Southwest monsoon with the average wind speed ranging between 2.3 and 2.7 m/s.

The flow in the catchment is seasonal. The streamflow only occurs about 8 months/year (typically from September to April of the following year) (Hai et al. 2018). Until now, there is a lack of official flow data in the catchment due to the absence of the hydrological station. This has created knowledge gaps for water resources planning in the La Vi catchment, whose water resources have been important for agricultural production (People's Committee of Binh Dinh Province 2018).

Agriculture is the dominant economic activity of the La Vi catchment with the area of agricultural land accounting for around 40%. In the structure of agricultural production, cultivation plays a key role with the main crops including

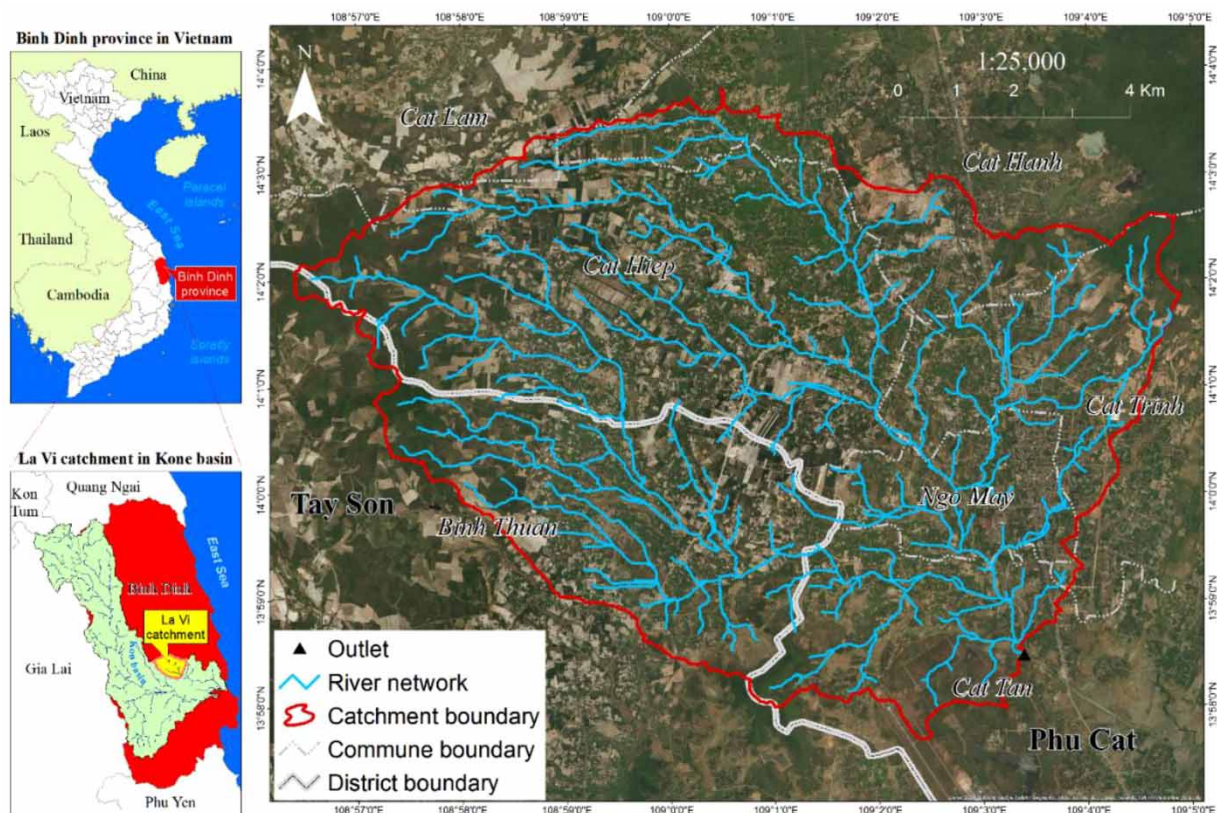


Figure 1 | Geographic location of the La Vi catchment.

rice, peanuts, and cassava. These crops are all grown in the dry season because this period combines favorable conditions for plants in terms of light intensity, air temperature, and rainfall.

The population data in the La Vi catchment were extracted from the Gridded Population of World Version 4 (Center for International Earth Science Information Network – Columbia University 2018), whereby the population size in this catchment increased by 1,121 people, from 31,506 people (2000) to 32,627 people (2020), with an average population growth rate of 0.18%/year. Average population density is about 261.01 people per km² (2020). Most people are concentrated in the East and North of the catchment.

Slope-area method

The slope-area method is used where there have not been measurements of discharge to provide a rating curve (Fenton & Keller 2001). It uses cross-sectional information and the Manning or Chézy friction laws, together with slope, to calculate the discharge approximately. Manning (1891) modified Chezy's equation resulting in an empirically preferable equation:

$$Q = \frac{1}{n} AR^{\frac{2}{3}} S^{\frac{1}{2}} \quad (1)$$

where Q is the discharge (m³/s), n is Manning's roughness (s/m^{1/3}), A is the cross-sectional area of the flow perpendicular to the flow direction (m²), R is the hydraulic radius (m) = A/P with P is the wetted perimeter of cross-sectional flow area (m) and S is the bottom slope of channel, m/m (dimensionless).

For the method to be valid, a reach must be carefully selected such that uniform flow conditions are approximated (Gordon et al. 2004). This means that the width and depth of flow, the water velocity, the streambed materials, and the channel slope remain constant over a straight reach, and further, that the channel slope and water slope are parallel. A straight, fairly homogeneous reach should be selected with a length at least five times the mean width (Dackombe & Gardiner 1983). Surveyed information is used to calculate the values of A and R . The slope, S , is

actually the slope of the energy line. However, in practice, the energy slope is assumed parallel to the water surface slope and the bed slope. The more closely the reach approximates uniform conditions, the better the results. The last variable is Manning's n , which is a composite factor that accounts for the effects of many forms of flow resistance. In a reach where the slope is uniform and the roughness of the bed and banks is similar (e.g., an artificial channel), Manning's n can usually be assumed to be a constant. Estimates of Manning's n can be made by choosing a value from a table such as Supplementary Appendix Table A1.

SWAT model

SWAT is a public domain hydrological model developed at the United States Department Agricultural Research Service during the early 1970s (Neitsch et al. 2011). The model is used to simulate the quality and quantity of surface and groundwater and predict the environmental impact of land use, land management practices, and climate change at small watershed and river basin scales on daily time step, monthly, or even annually. To satisfy this objective, it is physically based, and hence it requires extensive physical parameters to represent the real hydrological processes in the catchment. One benefit of this approach is ungauged basins can be modeled. The SWAT model divided a watershed into multiple sub-basins, which are further discretized into units of unique slope/soil/land use characteristics called hydrological response units (HRUs). The hydrologic components such as evapotranspiration, surface runoff, groundwater flow, and sediment yield are estimated separately for each HRU, which are then summarized for each sub-basin and the whole watershed.

The water balance in SWAT is given as follows (Neitsch et al. 2011):

$$SW_t = SW_o + \sum_{i=1}^t (R_{\text{day}} - Q_{\text{surf}} - E_a - w_{\text{seep}} - Q_{\text{gw}}) \quad (2)$$

where SW_t is the final soil water content (mm), SW_o is the initial soil water content on day i (mm), t is the time (days), R_{day} is the amount of precipitation on day i (mm), Q_{surf} is the amount of surface runoff on day i (mm), E_a is

the amount of evapotranspiration on day i (mm), w_{seep} is the amount of water entering the vadose zone from the soil profile on day i (mm), and Q_{gw} is the amount of groundwater runoff on day i (mm).

Methodology

The implementation process of the study was divided into four parts (see Figure 2): (1) collecting weather data by IoT-based automatic meteorological station, rainfall gauge, and surface meteorological station, (2) calculating discharge in the La Vi catchment based on river morphology data, water level data, and discharge measurements using the slope-area method, (3) calibration and validation of the SWAT model for discharge based on river morphology data, topographic map, 2015 land-use map, soil map, weather data, and estimated discharges of the slope-area method, and (4) water resources assessment of the catchment in terms of blue and green water (Falkenmark & Rockström 2006; Schuol et al. 2008).

The performance of the slope-area method and SWAT model in simulating discharge was evaluated by using

three statistics quantitative indices, including Nash–Sutcliffe index (NSI), percent bias (PBIAS), and coefficient of determination (R^2). The performance ratings for these indices are shown in Table 1.

Data acquisition

The input data, including discharge, water level, weather, river morphology, topographic map, 2015 land-use map, and soil map, were collected from many different sources. A detailed description of input data is shown in Table 2.

Table 1 | Performance ratings for statistics quantitative indices for watershed-scale models

Index	Performance rating		
	Satisfactory	Good	Very good
NSI ^a	$0.50 < \text{NSI} \leq 0.70$	$0.70 < \text{NSI} \leq 0.80$	$\text{NSI} > 0.80$
PBIAS (%) ^b	$\pm 15 \leq \text{PBIAS} < \pm 25$	$\pm 10 \leq \text{PBIAS} < \pm 15$	$\text{PBIAS} < \pm 10$
R^{2a}	$0.60 < R^2 \leq 0.75$	$0.75 < R^2 \leq 0.85$	$R^2 > 0.85$

^aMoriasi et al. (2015).

^bMoriasi et al. (2007).

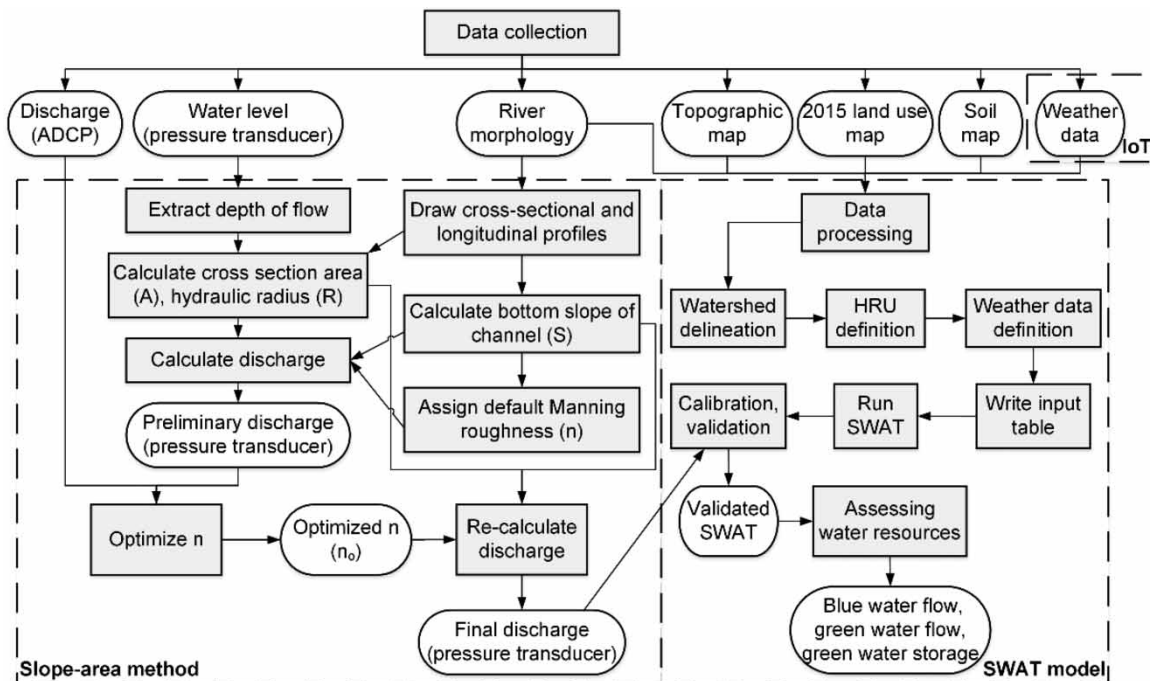


Figure 2 | Flowchart diagram of methodology.

Table 2 | The input data

ID	Data type	Description	Source
1	Discharge	Recorded at the upstream side of Tan Hoa bridge (1, 21, 22 December 2015, 16 January 2016) using ADCP; Observed variable: Discharge	Central Vietnam Division for Water Resources Planning and Investigation
2	Water level	Recorded at the upstream side of Tan Hoa bridge (13 November 2015–28 May 2016, 21 January 2017–9 February 2018) using pressure transducer; Observed variable: Water level (20 min time step)	Central Vietnam Division for Water Resources Planning and Investigation
3	Weather	Recorded at the automatic meteorological station on Xom Tay bridge (2016–2017) in MS Excel format; Observed variable: Air temperature, Relative humidity, Rainfall (hourly time step) Recorded at Phu Cat rainfall gauge (1998–2017) in MS Excel format; Observed variables: Rainfall (daily time step) Recorded at Quy Nhon surface meteorological station (1990–2017) in MS Excel format; Observed variables: Air temperature, Relative humidity, Sunshine hour, Wind speed (daily time step)	Nong Lam University, Ho Chi Minh City South Central Hydro-Meteorological Centre South Central Hydro-Meteorological Centre
4	River morphology	Derived from hydrographic survey along main rivers and at the upstream side of Tan Hoa bridge; Observed variables: Cross-sectional and longitudinal profiles	Central Vietnam Division for Water Resources Planning and Investigation
5	Topographic map	Microstation format, scale 1:10,000	Binh Dinh Department of Natural Resources and Environment
6	2015-land use map	Microstation format, scale 1:25,000	Binh Dinh Department of Natural Resources and Environment
7	Soil map	MapInfo format, scale 1:100,000	Central Sub-Institute of Agricultural Planning and Design

The discharge data recorded at the upstream side of Tan Hoa bridge using acoustic doppler current profiler (ADCP) (see Supplementary Appendix Figure A1b) was provided by Central Vietnam Division for Water Resources Planning and Investigation. Due to the danger of flood flow in the catchment, discharge only was sporadically measured at the end of the wet season of 2015 (1, 21, 22 December 2015) and at the beginning of the dry season of 2016 (16 January 2016).

The water level data recorded at the upstream side of Tan Hoa bridge using pressure transducer (see Supplementary Appendix Figure A1c) were provided by Central Vietnam Division for Water Resources Planning and Investigation. Water level was measured continuously from 13 November 2015 to 9 February 2018 every 20 min. Unfortunately, due to equipment failure, there was missing data during the period between 29 May 2016 and 20 January 2017.

Weather data were collected by the automatic meteorological station, rainfall gauge, and surface meteorological station (see Supplementary Appendix Figure A1a and A1d). On Xom Tay bridge, an IoT-based automatic meteorological station was designed and installed by Nong Lam University, Ho Chi Minh City, in late 2015 to record hourly weather data between 2016 and 2017. This weather station contained a DHT11 sensor to monitor air temperature, relative humidity, and a raindrop sensor to detect rainfall. All sensors were connected to an Arduino Uno, which was the main processing unit for the entire system. In turn, Arduino Uno retrieved, analyzed, and observed data from the sensors. The processed data were then uploaded and stored in a website using NodeMCU and Ubidots. At the same time, the study collected daily rainfall data at the Phu Cat station provided by South Central Hydro-Meteorological Centre during the period from 1998 to 2017. In addition, the study also used daily weather data including air temperature, relative

humidity, sunshine hour, and wind speed at the Quy Nhon surface meteorological station provided by South Central Hydro-Meteorological Centre in the period from 1990 to 2017.

River morphology data along main rivers and at the upstream side of Tan Hoa (see Supplementary Appendix Figure A2) were created by Central Vietnam Division for Water Resources Planning and Investigation. Two observed variables were cross-sectional and longitudinal profiles.

Both a topographic map and 2015 land-use map of Binh Dinh province in Microstation format were provided by Binh Dinh Department of Natural Resources and Environment. Meanwhile, the soil map of Binh Dinh province in MapInfo format was provided by Central Sub-Institute of Agricultural Planning and Design.

River cross-sectional and longitudinal profiles

Based on river morphology data at the upstream side of Tan Hoa bridge, cross-sectional and longitudinal profiles are drawn in Supplementary Appendix Figure A3 and A4, respectively, in which the river cross-section has a non-isosceles trapezoid shape. The banks are quite high to control high waters. The riverbed during the measurement period has changed a lot due to the reconstruction of the bridge. Our field observations determined that the material composition of the riverbed at Tan Hoa bridge is mainly sand, gravel, and mud. Eucalyptus trees are planted on the left bank, while acacia trees are planted on the right bank. With these geomorphologic characteristics (see Supplementary Appendix Table A1) the study used three Manning's n values of 0.035, 0.0675, and 0.100 to estimate discharge.

In another aspect, for longitudinal profile, the riverbed at Tan Hoa bridge is relatively flat with small elevation variations. The average value of the channel bottom slope at the bridge was estimated to be 0.6 m/1 km.

Hydraulic characteristics and estimated preliminary discharges

Hydraulic characteristics and estimated preliminary discharges at the upstream side of Tan Hoa bridge are shown in Supplementary Appendix Table A2 and Figure A5. For

every possible water level (in 50 cm steps), cross-sectional area, hydraulic radius, and discharge were calculated corresponding to three given Manning's n values.

Optimized Manning's n value

A simple spreadsheet methodology is used for Manning's roughness (n) parameter estimation of the slope-area method. The optimization model may be written as follows:

Maximize,

$$NSI = 1 - \frac{\sum_{t=1}^6 (Q_s^t - Q_o^t)^2}{\sum_{t=1}^6 (Q_o^t - \overline{Q_o})^2}$$

Subject to,

$$0 \leq n \leq 1$$

where Q_s is the estimated discharge from water level data measured by pressure transducers using Equation (1) (m^3/s), Q_o is the observed discharge by ADCP (m^3/s), $\overline{Q_o}$ is the mean of observed discharges by ADCP, t is the time, and n is Manning's roughness ($s/m^{1/3}$).

The optimal solution showed very good results for all of the indices ($NSI = 0.82$, $PBIAS = -3.46$, $R^2 = 0.88$) as shown in Supplementary Appendix Figure A6. The optimized value of n at the upstream side of Tan Hoa bridge reached 0.1356.

SWAT model input

The digital elevation model (DEM) (see Supplementary Appendix Figure A7) in GeoTIFF format with 5 m spatial resolution was interpolated using a topographic map and river longitudinal profiles. The 2015 land-use map was classified into seven categories (see Supplementary Appendix Figure A8), including paddy rice (RICE, 18.3%), other annual plants (AGRR, 16.4%), perennial plants (AGRC, 10.7%), evergreen forest (FRSE, 21.4%), built-up land (URBN, 31.7%), bare land (BARR, 0.4%), and water body (WATR, 1.1%). The soil map was classified into seven types (see Supplementary Appendix Figure A9), including

Cambic Fluvisols (0.5%), Dystric Gleysols (2.8%), Haplic Acrisols (36.4%), Lithic Leptosols (1.2%), Rhodic Acrisols (48.7%), Rhodic Ferralsols (8.2%), and Xanthic Ferralsols (2.2%), with physical and chemical properties required by the SWAT model. Weather data were classified into two categories: weather generator data (Quy Nhon station) and weather input data (Xom Tay station, Phu Cat rainfall gauge, and Quy Nhon station).

SWAT model setup

The SWAT model setup was carried out using ArcSWAT 2012 interface in ArcGIS Desktop software. The La Vi catchment was delineated and divided into 121 sub-catchments based on the DEM, which are presented in Supplementary Appendix Figure A10. HRUs were created using a combination of 10% land use over sub-catchment area, 10% soil class over land use area, and 10% slope class over soil area. With these combinations, 1,121 HRUs were defined. Weather data including precipitation, minimum and maximum air temperature, relative air humidity, solar radiation, and wind speed for the period of 1998–2017 were imported in the SWAT model. Finally, the SWAT was run on daily time step to simulate hydrological processes for a period of 20 years (1998–2017) with the first two years as a warm-up.

RESULTS AND DISCUSSION

Estimated discharges in the La Vi catchment

Discharges were estimated at the upstream side of Tan Hoa bridge every 20 min using the slope-area method with optimized $n = 0.136$ as shown in Figure 3. It can be seen that dry season flow was low with the discharge value ranging from 1.7 to 20.5 m³/s, equivalent to 0.76–1.79 m water depth. At the beginning of the flood season, the flow continued to remain low with a discharge value of about 2.8 m³/s (approximately 1 m water depth). However, in the middle and end of the flood season when heavy rains often appear, the flow increased rapidly. Discharge reached over 200 m³/s (equivalent to water depth above 3.8 m) in the two extreme floods that occurred in November and December 2017.

Besides seasonal variation due to the impact of rainfall, the flow regime in the catchment has also been affected by anthropogenic factors. Cay Tram weir was constructed about 2.5 km downstream of Tan Hoa bridge with the function of preventing seawater intrusion and maintaining water level in the river during the dry season (see Figure 4). The weir is closed when the river stage is drop-down due to no rainfall. It caused a rise in the river stage to be a certain level. When heavy rainfall happened, the weir was opened

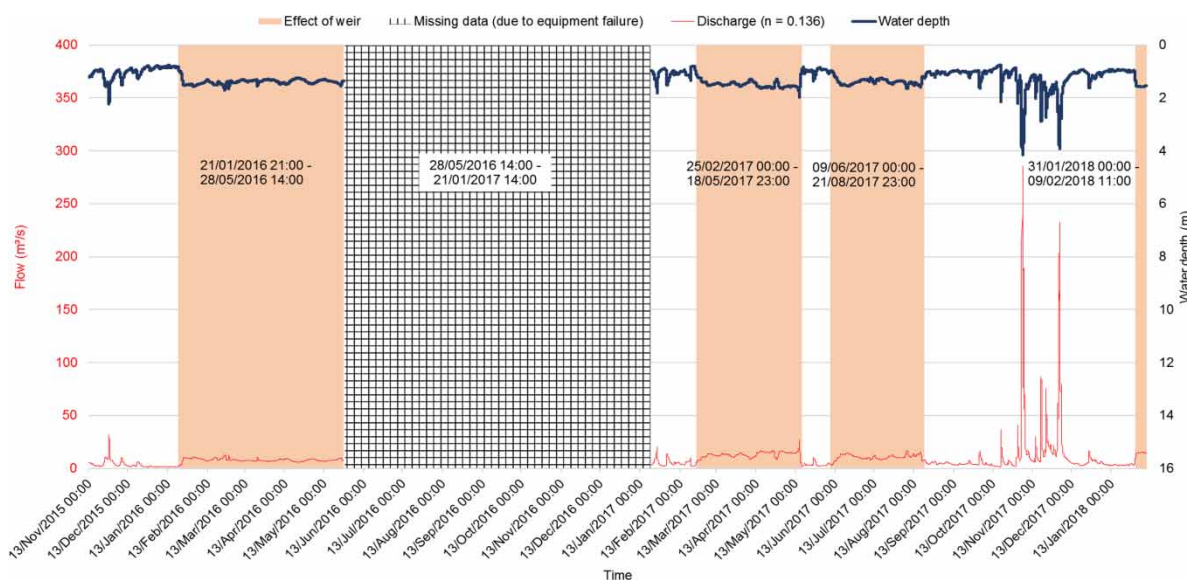


Figure 3 | Estimated discharges ($n = 0.136$) every 20 min at the upstream side of Tan Hoa bridge during from November 2015 to February 2018.

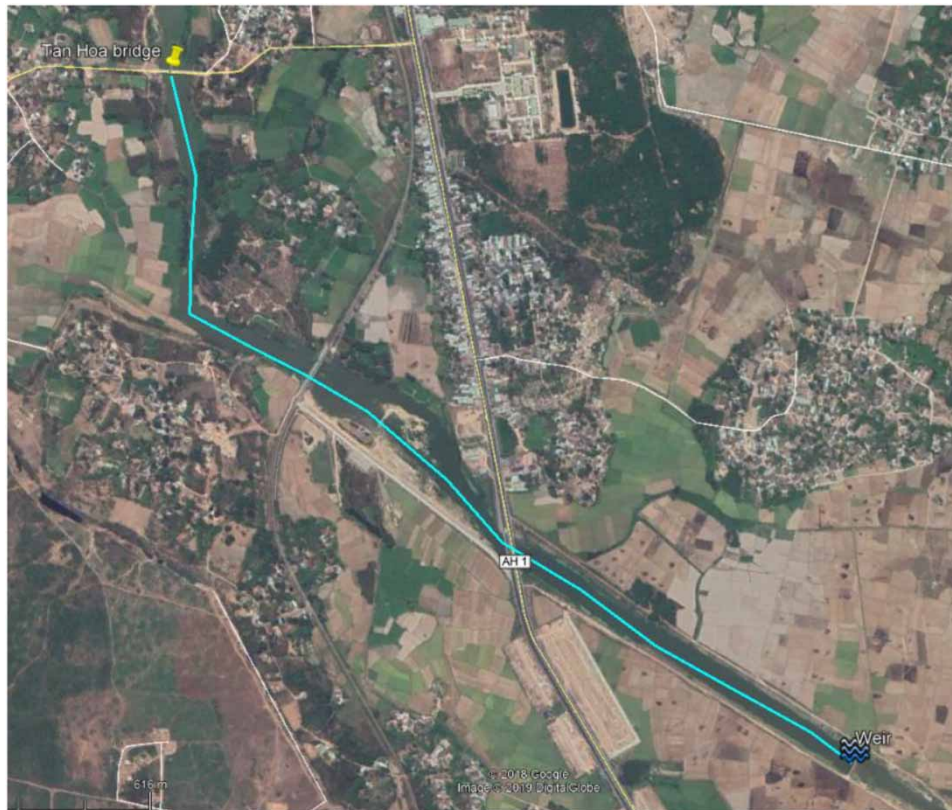


Figure 4 | Location of Cay Tram weir at the downstream side of Tan Hoa bridge.

for river water getting through. In the study, based on water level time series data during the period 2016–2018, the weir operation altered the water depth of the river, estimated to increase by about 0.6–1 m.

The periods when the weir affected river stage were determined, including the dry seasons of 2016 (21 January–28 May), 2017 (25 February–18 May, 9 June–21 August), and 2018 (31 January–9 February). The estimated discharges by the slope-area method in the above stages were discarded and not used to calibrate and validate the SWAT model.

Calibration and validation of the SWAT model

Based on the performance of the SWAT model in simulating daily discharge at the upstream side of Tan Hoa bridge (see Figure 5) and the guidelines summarized by Abbaspour et al. (2015), nine relevant parameters were selected for model calibration as in Table 3. Figures 6 and 7 show the simulated

and observed daily discharges at the upstream side of Tan Hoa bridge in the calibration and validation periods, respectively. The 95% prediction uncertainty (95PPU), which expressed uncertainties in SWAT model output variables, is calculated at the 2.5 and 97.5% levels of the cumulative distribution of an output variable generated by the propagation of the parameter uncertainties using Latin hypercube sampling (Abbaspour 2015). The overall performance of the model has satisfactory results for both calibration (NSI = 0.58, PBIAS = -22.7, $R^2 = 0.68$) and validation (NSI = 0.87, PBIAS = 20.0, $R^2 = 0.89$) periods.

During the 70-day calibration period (13 November 2015 to 31 December 2015), compared with the observed discharge values, most of the simulated flood peaks were higher and occurred 1–2 days earlier. Based on the baseflow filtering algorithm with a filter parameter of 0.925, baseflow was separated from water discharge. The simulated base flows were about 0.5–2 m³/s higher than the observed ones. During the 132-day validation period (22 August

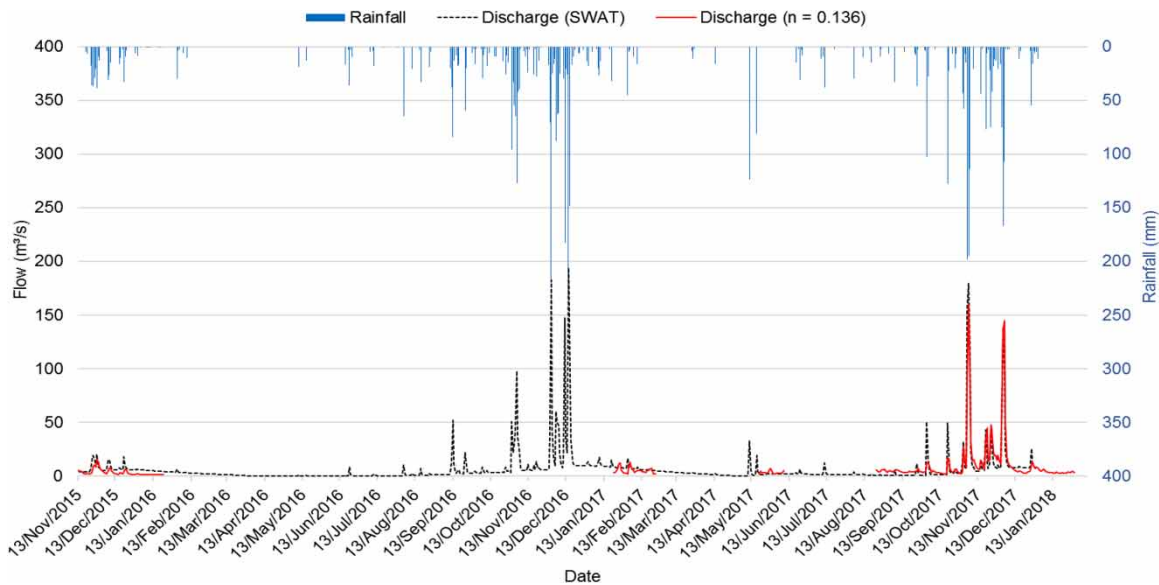


Figure 5 | Comparison of simulated (SWAT model) and observed (slope-area method, $n = 0.136$) discharge at the upstream side of Tan Hoa bridge on daily time step.

Table 3 | Fitted values of SWAT calibration parameters and their sensitivity

Parameters	Definition	t-stat	p-value	Initial range	Final range	Fitted value
HRU_SLP.hru	Average slope steepness	7.99	0.00	r (-2,0)	(-1.20, 0.42)	-0.39
OV_N.hru	Manning's 'n' value for overland flow	-3.10	0.00	r (0,2)	(0.88, 2.66)	1.77
SOL_AWC(.).sol	Available water capacity of the soil layer	2.55	0.01	r (0,2)	(-0.24, 1.26)	0.51
GW_REVAP.gw	Groundwater 'revap' coefficient	2.51	0.01	r (0,2)	(0.73, 2.21)	1.47
ESCO.hru	Soil evaporation compensation factor	-2.03	0.04	r (0,2)	(0.86, 2.60)	1.73
CN2.mgt	SCS runoff curve number for moisture condition I	1.93	0.06	r (-2,2)	(-1.05, 0.87)	-0.09
REVAPMN.gw	Threshold depth of water in the shallow aquifer for 'revap' to occur (mm)	-1.44	0.15	r (-2,0)	(-1.40, -0.18)	-0.79
SLSUBBSN.hru	Average slope length	-1.38	0.17	r (0,2)	(-0.63, 1.13)	0.25
GWQMN.gw	Threshold depth of water in the shallow aquifer required for return flow to occur (mm)	-0.46	0.64	r (0,2)	(0.60, 1.82)	1.21

Note: r_ means the existing parameter value is multiplied by (1+ a given value), t-stat provides a measure of sensitivity (larger absolute values are more sensitive), and p-value determined the significance of the sensitivity (a value close to zero has more significance).

2017 to 31 December 2017), the simulation of discharge was better although the model underestimated the base flows and flood peaks.

Blue and green water resources in the La Vi catchment

Blue water, or blue water flow, is the sum of water yield and deep aquifer recharge. Green water includes green water

flow (actual evapotranspiration) and green water storage (soil moisture content). In this study, we used the output variables WYLD (Water yield), ET (Actual evapotranspiration from the sub-basin), and SW (soil water content) in the output.sub file of the SWAT model to calculate blue water flow, green water flow, and green water storage, respectively. In addition, the green water coefficient was used to account for the relative importance of blue water

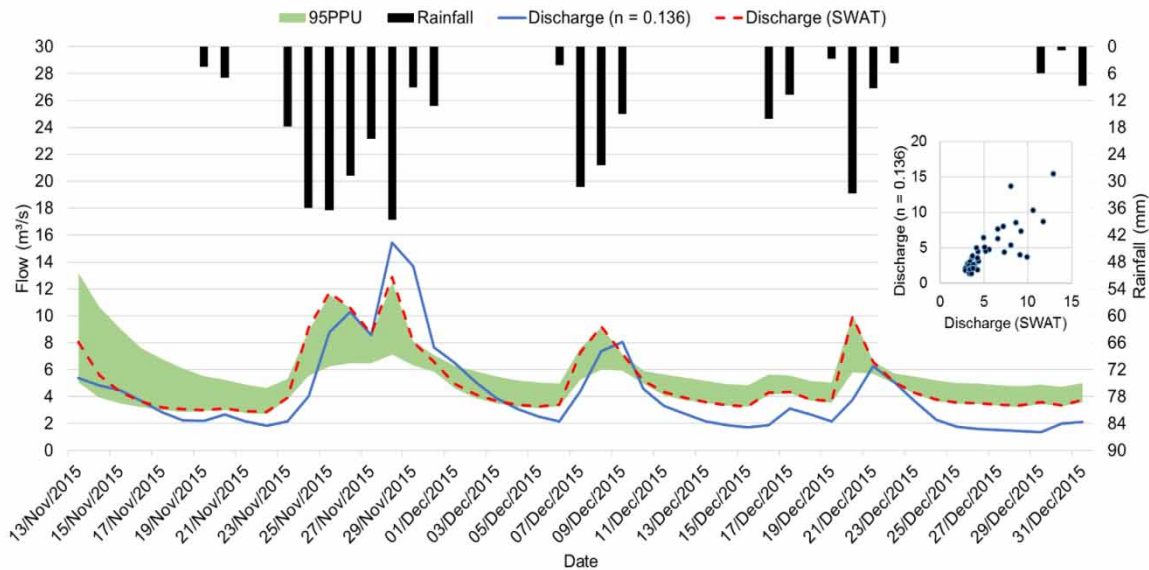


Figure 6 | Simulated (SWAT model) and observed (slope-area method, $n = 0.136$) daily discharge at the upstream side of Tan Hoa bridge for the calibration period.

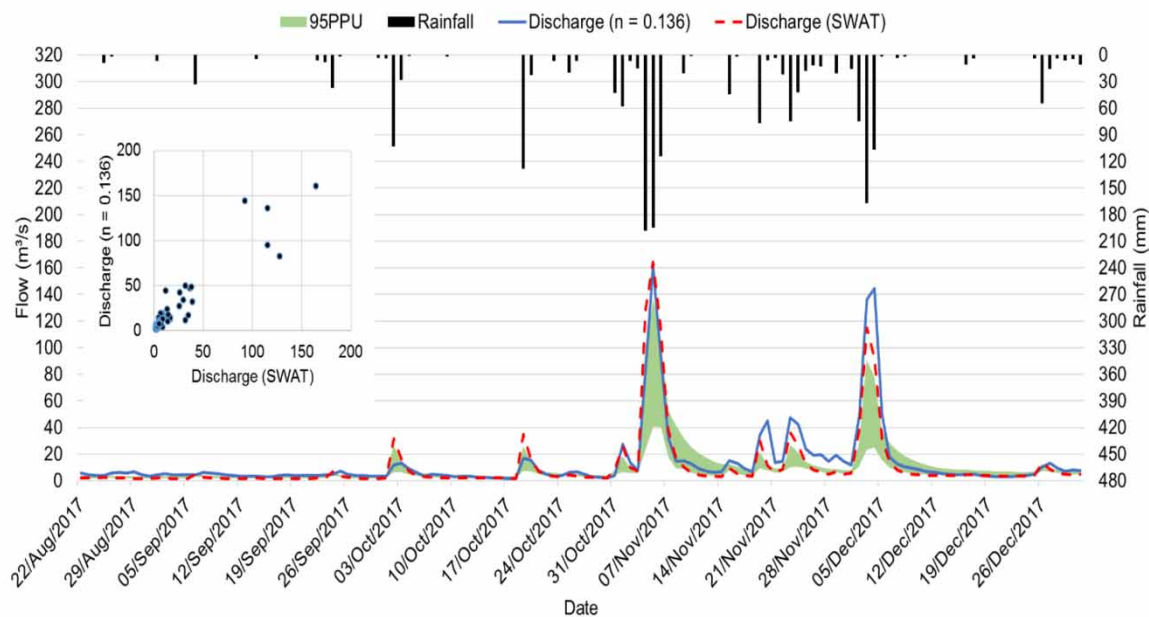


Figure 7 | Simulated (SWAT model) and observed (slope-area method, $n = 0.136$) daily discharge at the upstream side of Tan Hoa bridge for the validation period.

flow and green water flow, which is defined as the ratio of green water flow to the total green and blue water flows (Chen et al. 2015).

The changes in blue water flow, green water flow, green water storage, and green water coefficient between 2000 and

2017 are presented in Figure 8. The annual average of blue water flow, green water flow, and green water storage in the La Vi catchment reached 1,596.50, 371.13, and 15.36 mm, respectively. The variation coefficients were 0.28, 0.14, and 0.31 for blue water flow, green water flow,

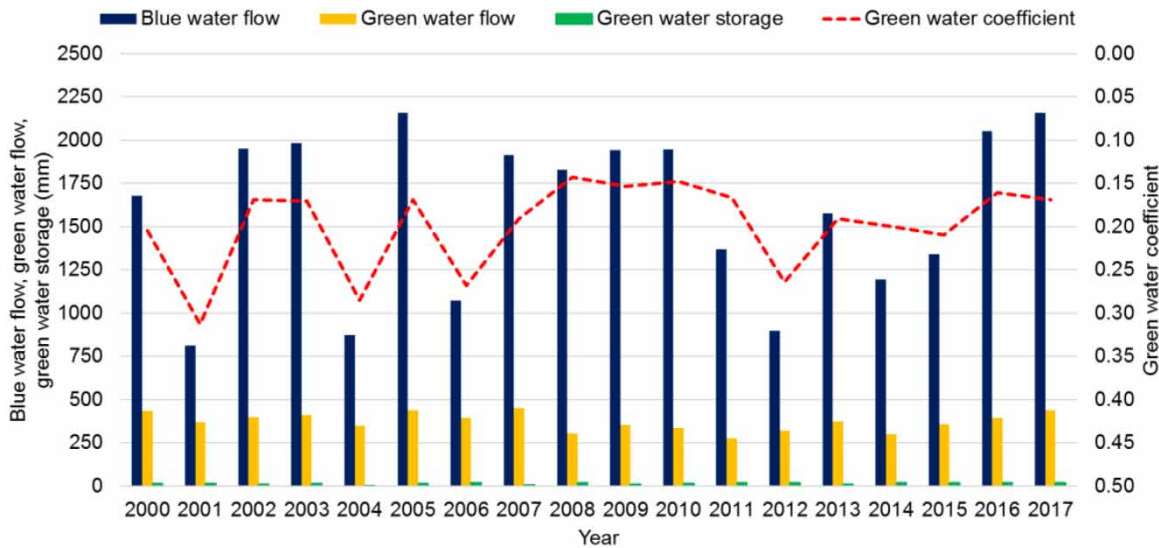


Figure 8 | Temporal variation of blue water flow, green water flow, green water storage, and green water coefficient from 2000 to 2017.

and green water storage, respectively. This means that the change of green water flow was relatively more stable than blue water flow and green water storage. Moreover, green water flow only contributed about 0.14–0.31 to the total water flow of the La Vi catchment.

The value of slope estimates β and trend statistic Z in the Mann–Kendall test for annual blue water flow, green water flow, and green water storage in the La Vi catchment from 2000 to 2017 are shown in Table 4. Both blue water flow and green water storage showed an increasing trend of 13.73 and 0.39 mm/year, respectively. In contrast, green water flow tends to decrease by 3.38 mm/year.

The spatial variation of annual average blue water flow, green water flow, green water storage, and green water coefficient is shown in Figures 9–12, respectively. It is clear that the spatial distribution of the blue water flow was uneven. The blue water flow reached a higher value in the center

of the catchment, with blue water flow more than 1,600 mm/year.

Compared with blue water flow, the spatial distribution of green water flow was more homogeneous. The green water flow in most parts of the catchment varied from 330 to 380 mm/year. The high-value areas of green water flow were mainly distributed in the western upstream of the catchment and the riverside downstream areas.

For green water storage, the value ranged between 12 and 27 mm/year. However, there was a contrast between the central region and other areas of the catchment. High green water storage concentrated in the east and west. Meanwhile in the central region, green water storage was low.

Considering its relative importance, the green water flow contributed less than a quarter of the total flow, except for a few sub-catchments near the downstream catchment. The value of green water coefficient was mainly in the range of 0.17–0.20.

Table 4 | The Mann–Kendall test for annual blue water flow, green water flow, and green water storage in the La Vi catchment from 2000 to 2017

Water resource variable	β (mm/year)	Z
Blue water flow	13.73	0.53
Green water flow	−3.38	−0.91
Green water storage	0.39	1.89 ⁺

Note: (†) means significant at $p = 0.1$, β is slope estimates, and Z is trend statistic in the Mann–Kendall test.

DISCUSSION

The La Vi catchment has a long dry season that is identical to a semi-arid area. Two dominant soil types in the catchment are Haplic Acrisols and Rhodic Acrisols with soil texture of sand, loamy sand, or sandy loam, which has low

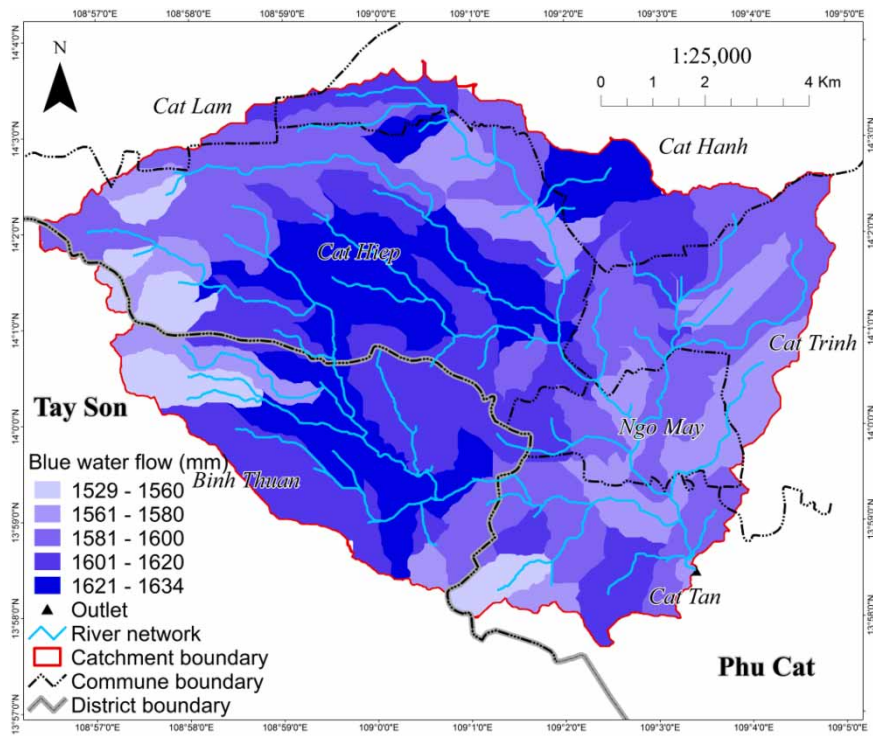


Figure 9 | The spatial distribution of annual blue water flow (2000–2017).

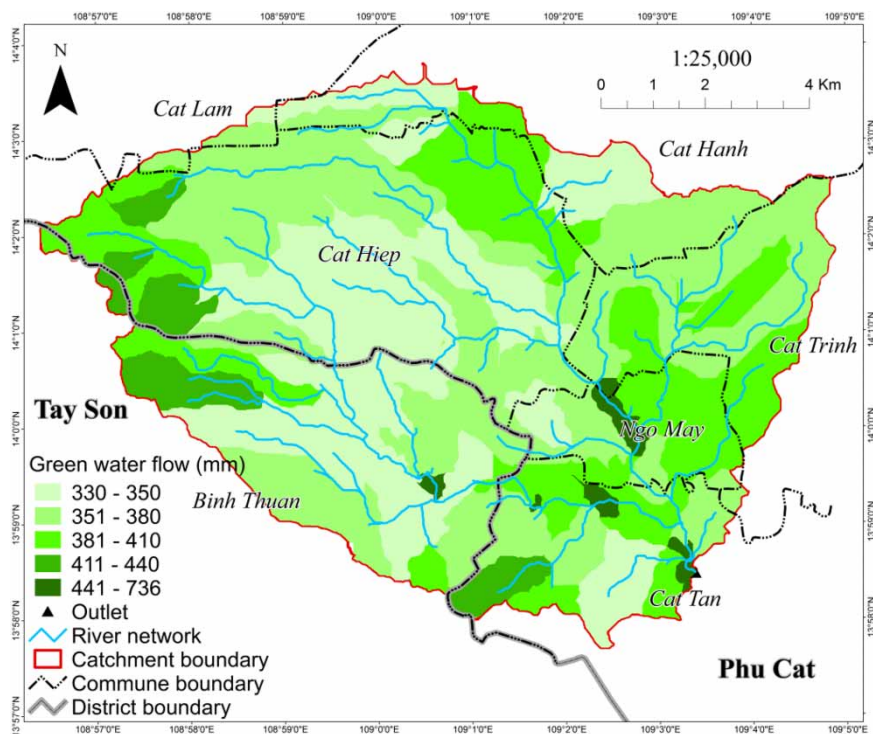


Figure 10 | The spatial distribution of annual green water flow (2000–2017).

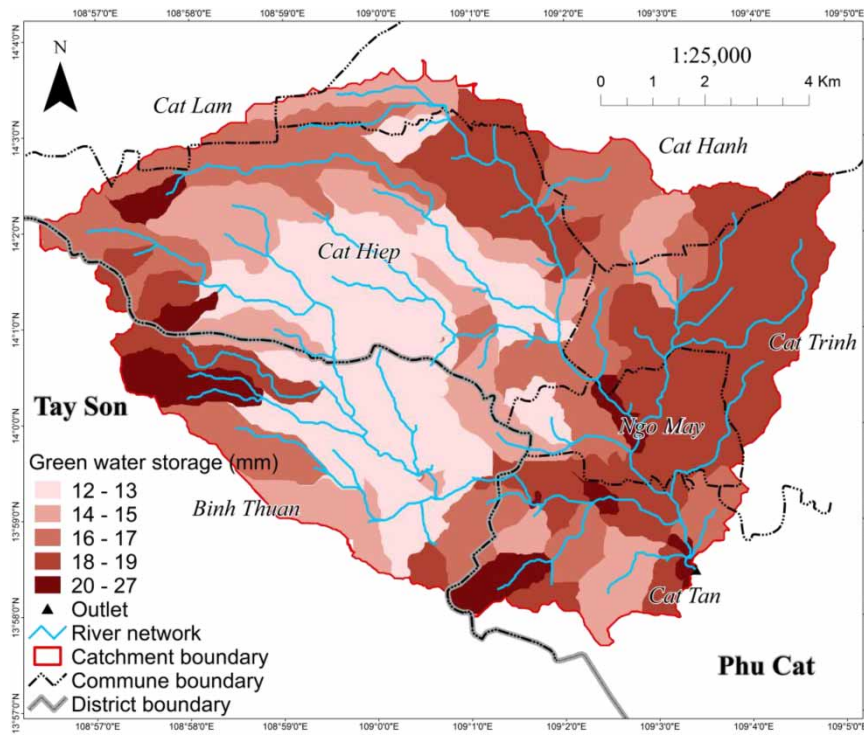


Figure 11 | The spatial distribution of annual green water storage (2000–2017).

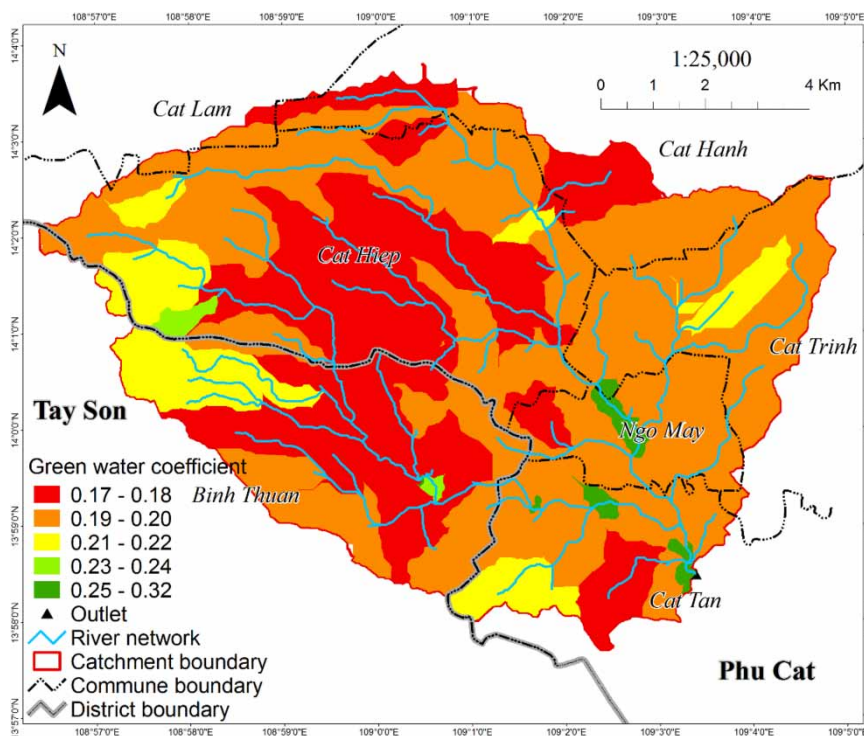


Figure 12 | The spatial distribution of annual green water coefficient (2000–2017).

runoff potential and high infiltration rates. This leads to a strong contrast of natural streamflow between non-flood and flood seasons. In general, the peak flow of two seasons varies about 70 times. This result shows that people in the basin are exposed annually to water-related disasters such as droughts and floods.

The operation of Cay Tram weir located downstream is an effective structural solution that contributes to reducing droughts and floods. In the dry season, it prevents seawater intrusion, regulates irrigation water for agricultural production, and stabilizes groundwater for domestic needs. Moreover, it drains floods quickly in the wet season.

Water resources in the basin are mainly contributed by blue water flow with more than 70% and concentrated distribution in the center of the catchment. It means the construction of irrigation structures should be prioritized in these areas. Green water flow was relatively stable over time. In contrast, green water storage showed an increasing trend. The high-value areas of green water flow and green water storage were observed in the western upstream and the riverside downstream. It brings advantages of forestry development and rain-fed crop production in these regions.

Compared with previous studies, the novelty of our study lies in applying IoT technology for meteorological monitoring to improve the availability and continuity of weather data in the La Vi ungauged basin. This allows us to detect significant differences in the local climate of the catchment compared with Quy Nhon meteorological station as well as provide detailed meteorological data for hydrological simulation in the catchment. Owing to its compactness, high accuracy, low price, and easy customization, IoT-based weather stations can be easily deployed in other basins of Vietnam regardless of terrain and weather conditions. Besides, we use a systematic approach to separately analyze the two components of water resources as blue water and green water in terms of space and time. Since then, identifying emerging water issues, analyzing existing solutions, and proposing feasible solutions can enable sustainable use of water resources in the catchment. The above approach was implemented through SWAT, a semi-distributed and free-of-charge model that has been used in Vietnam.

Limitations of this study are related to SWAT. Firstly, we have not been able to accurately restore streamflow when Cay Tram weir was operating. The reason is that SWAT is

a one-dimensional hydrological model, not suitable for areas affected by tides or surges due to weirs. To overcome this limitation, hydraulic models could be integrated. In addition, because SWAT is a continuous model, it needs to be calibrated and validated for the long term in order to improve model performance. This could be done by using evapotranspiration and crop yield of remote sensing data. Finally, this study has not considered groundwater in the saturated zone, an important water source during the dry season in the catchment. Therefore, further research should couple MODFLOW and SWAT to enhance the simulation ability of water resources in the catchment.

CONCLUSIONS

Quantifying water resources is a major challenge for hydrologists in developing countries where a large number of watersheds are ungauged. Thanks to the installation of the IoT-based automatic meteorological station, we have improved the availability and continuity of weather data in the La Vi ungauged basin.

Estimated discharges at the upstream side of Tan Hoa bridge every 20 min from November 2015 to February 2018 by the slope-area method showed not only the significant differences in streamflow between the dry season and wet season but also the impact of weir located downstream the La Vi catchment. The peak flow in the flood season can be 70 times higher than that in the non-flood season. The operation of Cay Tram dam downstream causes an increase in river water level and reduces hydraulic gradient resulting in a decrease in flow to the river during dry periods.

The annual average of blue water flow, green water flow, and green water storage in the La Vi catchment was estimated by the well-validated SWAT model during the period 2000–2017. The blue water flow reached a higher value in the center of the catchment. Meanwhile, the high-value areas of green water flow and green water storage were in the western upstream and the riverside downstream.

The study contributes insights into the flow regime and water budget in the La Vi catchment at both spatial and temporal scales. It could provide significant information for efficiently utilizing and allocating the water resources as well as sustainable agricultural development in the region.

The calibrated SWAT model in this study provides a strong basis for forthcoming studies in the catchment regarding agricultural land use change, climate change impact, and irrigation system planning.

The limitations of this study are related to the SWAT model nature and availability of the input data. To overcome these challenges, it is necessary to integrate the SWAT model with hydraulic models, groundwater models and exploit remote sensing data.

ACKNOWLEDGEMENTS

We thank our colleagues from Research Centre for Climate Change, Nong Lam University, Ho Chi Minh City, for their assistance with the processing of the topographic map and soil map.

CONFLICTS OF INTEREST

The authors declare no conflict of interest.

AUTHORS CONTRIBUTIONS

All authors formulated the concept. L. D. N. collected, processed, analyzed, visualized data, and wrote the paper. P. D. N. D. edited the paper. L. K. N. supervised research and contributed ideas during the data analysis.

FUNDING

This research was funded by Australian Centre for International Agricultural Research through the project entitled 'Integrated water, soil and nutrient management for sustainable farming systems in South Central Coastal Vietnam and Australia' (Project code: SMCN/2012/069).

DATA AVAILABILITY STATEMENT

All relevant data are included in the paper or its Supplementary Information.

REFERENCES

- Abbaspour, K. C. 2015 *SWAT-CUP: SWAT Calibration and Uncertainty Programs – A User Manual*. Swiss Federal Institute of Aquatic Science and Technology, Eawag.
- Abbaspour, K. C., Rouholahnejad, E., Vaghefi, S., Srinivasan, R., Yang, H. & Kløve, B. 2015 *A continental-scale hydrology and water quality model for Europe: calibration and uncertainty of a high-resolution large-scale SWAT model*. *Journal of Hydrology* **524**, 733–752. <https://doi.org/10.1016/j.jhydrol.2015.03.027>.
- Ang, R. & Oeurng, C. 2018 *Simulating streamflow in an ungauged catchment of Tonlesap Lake Basin in Cambodia using Soil and Water Assessment Tool (SWAT) model*. *Water Science* **32** (1), 89–101. <https://doi.org/10.1016/j.wsj.2017.12.002>.
- Askar, M. K. & Al-Jumaily, K. K. 2008 A nonlinear optimization model for estimating Manning's roughness coefficient. In: *Twelfth International Water Technology Conference*, Alexandria, Egypt, pp. 1299–1306.
- Begou, J. C. 2016 *Hydrological Modeling of the Bani Basin in West Africa – Uncertainties and Parameters Regionalization*. University of Abomey-Calavi, Godomey, Benin.
- Center for International Earth Science Information Network – Columbia University 2018 *Gridded Population of the World, Version 4 (GPWv4): Population Density, Revision 11*. NASA Socioeconomic Data and Applications Center (SEDAC), Palisades, NY. <https://doi.org/10.7927/H49C6VHW> (accessed 01 March 2021).
- Chen, C., Hagemann, S. & Liu, J. 2015 *Assessment of impact of climate change on the blue and green water resources in large river basins in China*. *Environmental Earth Sciences* **74** (8), 6381–6394. <https://doi.org/10.1007/s12665-014-3782-8>.
- Dackombe, R. & Gardiner, V. 1983 *Geomorphological Field Manual*. George Allen & Unwin, London.
- Ding, Y., Jia, Y. & Wang, S. S. Y. 2004 *Identification of Manning's roughness coefficients in shallow water flows*. *Journal of Hydraulic Engineering* **130** (6), 501–510. [https://doi.org/10.1061/\(asce\)0733-9429\(2004\)130:6\(501\)](https://doi.org/10.1061/(asce)0733-9429(2004)130:6(501)).
- Dingman, S. L. & Bjerklie, D. M. 2005 Estimation of river discharge. In: *Encyclopedia of Hydrological Sciences* (M. G. Anderson, ed.). John Wiley & Sons, Ltd. <https://doi.org/10.1002/0470848944>.
- Falkenmark, M. & Rockström, J. 2006 *The new blue and green water paradigm: breaking new ground for water resources planning and management*. *Journal of Water Resources*

- Planning and Management* **132** (3), 129–132. [https://doi.org/10.1061/\(ASCE\)0733-9496\(2006\)132](https://doi.org/10.1061/(ASCE)0733-9496(2006)132).
- Fenton, J. D. & Keller, R. J. 2001 *The Calculation of Streamflow from Measurements of Stage. Cooperatiive Research Center for Catchment Hydrology*. Available from: <http://www.catchment.crc.org.au/pdfs/technical200106.pdf>.
- Gordon, N. D., McMahon, T. A., Finlayson, B. L., Gippel, C. J. & Nathan, R. J. 2004 *Stream Hydrology: An Introduction for Ecologists. Ecological Engineering*, 2nd edn. John Wiley & Sons Ltd. [https://doi.org/10.1016/0925-8574\(93\)90041-D](https://doi.org/10.1016/0925-8574(93)90041-D).
- Guiamel, I. A. & Lee, H. S. 2020 *Watershed modelling of the Mindanao River Basin in the Philippines using the SWAT for water resource management. Civil Engineering Journal (Iran)* **6** (4), 626–648. <https://doi.org/10.28991/cej-2020-03091496>.
- Hai, V. M., Margaret, S. & Okke, B. 2018 *Flux dynamics at the groundwater-surface water interface in a tropical catchment. Limnologica* **68**, 36–45. <https://doi.org/10.1016/j.limno.2017.06.003>.
- Heydari, M., Sadeghian, J., Faridnia, M. & Shabanlou, S. 2018 *Combination of gradually varied flow theory and simulated annealing optimization in of Manning roughness coefficient. Journal of Applied Research in Water and Wastewater* **9** (1), 381–388.
- Kha, D. D., Nhu, N. Y. & Anh, T. N. 2018 *An approach for flow forecasting in ungauged catchments – A case study for Ho Ho reservoir catchment, Ngan Sau River, Central Vietnam. Journal of Ecological Engineering* **19** (3), 74–79. <https://doi.org/10.12911/22998993/85759>.
- Manning, R. 1891 *On the flow of water in open channels and pipes. Transactions of the Institution of Civil Engineers of Ireland* **20**, 161–207.
- Mishra, H., Denis, D. M., Suryavanshi, S., Kumar, M., Srivastava, S. K., Denis, A. F. & Kumar, R. 2017 *Hydrological simulation of a small ungauged agricultural watershed Semrakalwana of Northern India. Applied Water Science* **7** (6), 2803–2815. <https://doi.org/10.1007/s13201-017-0531-7>.
- Moriassi, D. N., Arnold, J. G., Van Liew, M. W., Bingner, R. L., Harmel, R. D. & Veith, T. L. 2007 *Model evaluation guidelines for systematic quantification of accuracy in watershed simulations. American Society of Agricultural and Biological Engineers* **50** (3), 885–900.
- Moriassi, D. N., Gitau, M. W., Pai, N. & Daggupati, P. 2015 *Hydrologic and water quality models: performance measures and evaluation criteria. Transactions of the ASABE* **58** (6), 1763–1785. <https://doi.org/10.13031/trans.58.10715>.
- Neitsch, S. L., Arnold, J. G., Kiniry, J. R. & Williams, J. R. 2011 *Soil and Water Assessment Tool Theoretical Documentation Version 2009. Texas Water Resources Institute Technical Report No. 406. Texas A&M University System College Station, Texas.*
- Nwe, C. M. & Htun, Z. M. M. 2018 *A smart weather monitoring system using Internet of Things. International Journal of Scientific Engineering and Research* **6** (7), 26–29.
- Oo, H. T., Zin, W. W. & Thin Kyi, C. C. 2020 *Analysis of streamflow response to changing climate conditions using SWAT model. Civil Engineering Journal (Iran)* **6** (2), 194–209. <https://doi.org/10.28991/cej-2020-03091464>.
- People's Committee of Binh Dinh province 2018 *Decision No. 2584/QD-UBND on Approval of Water Resources Planning in Binh Dinh Province by 2025, Vision to 2035 – Content of Allocation and Protection of Surface Water Resources. Vietnam.*
- Quan, N. H. 2006 *Rainfall-Runoff Modeling in the Ungauged Can Le Catchment, Saigon River Basin. International Institute for Geo-Information Science and Earth Observation.*
- Rafiei Emam, A., Kappas, M., Linh, N. H. K. & Renchin, T. 2017 *Hydrological modeling and runoff mitigation in an ungauged basin of central Vietnam using SWAT model. Hydrology* **4** (1), 17. <https://doi.org/10.3390/hydrology4010016>.
- Rahut, Y., Afreen, R. & Kamini, D. 2018 *Smart weather monitoring and real time alert system using IoT. International Research Journal of Engineering and Technology* **5** (10), 848–854.
- Reshma, T., Reddy, K. V., Pratap, D. & Agilan, V. 2014 *Optimization of Manning's roughness coefficients for a watershed using multi-objective genetic algorithm. In International Conference on Modeling Tools for Sustainable Water Resources Management.*
- Schuol, J., Abbaspour, K. C., Yang, H., Srinivasan, R. & Zehnder, A. J. B. 2008 *Modeling blue and green water availability in Africa. Water Resources Research* **44** (7), 1–18. <https://doi.org/10.1029/2007WR006609>.
- Sefick, S. A., Kalin, L., Kosnicki, E., Schneid, B. P., Jarrell, M. S., Anderson, C. J. & Feminella, J. W. 2015 *Empirical estimation of stream discharge using channel geometry in low-gradient, sand-bed streams of the southeastern plains. Journal of the American Water Resources Association* **51** (4), 1060–1071. <https://doi.org/10.1111/jawr.12278>.
- Sisay, E., Halefom, A., Khare, D., Singh, L. & Worku, T. 2017 *Hydrological modelling of ungauged urban watershed using SWAT model. Modeling Earth Systems and Environment* **3** (2), 693–702. <https://doi.org/10.1007/s40808-017-0328-6>.
- Srinivasan, R., Zhang, X. & Arnold, J. 2010 *SWAT ungauged: hydrological budget and crop yield predictions in the upper Mississippi River Basin. Transactions of the ASABE* **53** (5), 1533–1546.
- Van Zuidam, R. A. 1986 *Aerial Photo Interpretation in Terrain Analysis and Geomorphologic Mapping. Smits Publishers, The Hague, Netherlands.*
- Vietnamese Government 2016 *Decision No. 90/QD-TTg on Approval of a Master Plan for National Natural Resources and Environment Monitoring Networks for 2016–2025, with a Vision to 2030. Vietnam.*

First received 10 December 2020; accepted in revised form 26 April 2021. Available online 17 May 2021